

EXPERIMENTAL TESTS ON GAUGE THEORIES*

BY G. BARBIELLINI

L.N.F. Istituto Nazionale di Fisica Nucleare and Visitor at CERN, Geneva**

(Received August 26, 1981)

After a brief review of the main features of the gauge theory of weak interactions, known as $SU(2)_L \times U(1)$, the up-to-date experimental situation is presented. In the charged current sector the μ^+ polarization measurement from the reaction $\bar{\nu}_\mu N \rightarrow \mu^+ X$ gives a general confirmation at large Q^2 of the gauge nature of the weak interaction. The neutral current weak interaction results from e^+e^- storage rings and in neutrino quark scattering are reviewed with particular attention to the measurement of the weak strength parameter $\sin^2 \theta_W$.

PACS numbers: 12.20.Hx

1. Introduction

Since the discovery of the weak neutral current in neutrino-“quark” interactions, the experimental evidence collected in favour of the validity of the so-called standard model is so large that it is widely justified to examine the recent high statistics experimental data in the light of the prediction of the $SU(2)_L \times U(1)$ theory of weak interactions.

The energy range that is spanned by the present data on weak interactions goes from the few electronvolts of the light polarization rotation in atomic physics to close to 40 GeV in the e^+e^- storage rings such as PETRA, the DESY electron accumulator, or the Stanford machine PEP.

For the youngest students of this school let me recall the main features of the standard model that the experiments aim to verify.

The $SU(2)_L \times U(1)$ theory is a gauge theory of the electroweak forces that requires a local symmetry in the lagrangian for phase transformation of the fields and a weak isospin symmetry for the charged and neutral leptons. The gauge symmetry and the Lorentz invariance of the fundamental spinors imply the vector (V) and axial vector (A) nature of the currents. The V-A nature of the charged weak currents is imposed according to the experimental observation.

* Presented at the XXI Cracow School of Theoretical Physics, Paszówka, May 29 — June 9, 1981.

** Address: EP Division, CERN, CH-1211 Geneva 23, Switzerland.

The fundamental fermions are doublet or singlet of the weak isospin as shown in Table I. The relation between isospin and helicity is very relevant for the construction of more ambitious theories such as the grand unifying theory GUT (see John Ellis lectures).

TABLE I

$I = 1/2$	$\begin{pmatrix} \nu_e \\ e \end{pmatrix}_L$	$\begin{pmatrix} u \\ d \end{pmatrix}_L$
$I = 0$	e_R	u_R, d_R

The same doublet-singlet pattern is repeated for higher values of the fermion masses (families or generations).

The two gauge symmetries in the $SU(2)_L \times U(1)$ have independent coupling constants g, g' but if one requires that the $SU(2)_L \times U(1)$ includes the electromagnetic interactions one is left with a single coupling constant. This is usually given under the form $\sin^2 \theta_w$ defined by the equations

$$e^2 = g^2 \sin^2 \theta_w, \quad e^{-2} = g^{-2} + g'^{-2}$$

which give

$$\sin^2 \theta_w = \frac{g'^2}{g'^2 + g^2}.$$

After this short reminder of the standard model I will first present the results of a recent experiment that check the very general features of the gauge theory of weak interactions, helicity conservation. In the second part of this lecture I will present the status of the measurement on the quantity $\sin^2 \theta_w$.

2. Charged-current interactions

We now consider the measurement of the polarization of the μ^+ from the reaction

$$\bar{\nu}_\mu N \rightarrow \mu^+ X.$$

A general property of the gauge theories is the V or A nature of the interaction. The V and A interactions conserve the helicity of the particles. The results that I will present on the μ^+ polarization measurement at large Q^2 ($Q^2 \simeq 10 \text{ GeV}^2$) prove that with good accuracy the weak interaction behaves as a gauge theory at this momentum transfer.

From the Turley lectures at this school we have learned how to build the beams and the detectors for the experimental investigation on neutrino-nucleon interactions, so I will recall only very briefly the principle of the experiment carried out by the CHARM Collaboration with the CERN SPS wide band neutrino beam.

The experiment uses both large neutrino detectors at the CERN SPS: the CERN-Dortmund-Heidelberg-Saclay (CDHS) Collaboration and the CERN-Hamburg-Amster-

dam-Rome-Moscow (CHARM) Collaboration neutrino detectors (Fig. 1). The CDHS detector is used as an instrumented target for $\bar{\nu}_\mu$ interactions, and the CHARM apparatus as a muon polarimeter. The target detector consists of 19 magnetized iron toroids (total weight 1200 tons) interspersed with scintillator planes and drift chambers. The kinematical parameters (E_x , \vec{p}_μ) of the $\bar{\nu}_\mu$ interaction are measured in this detector. The toroidal field

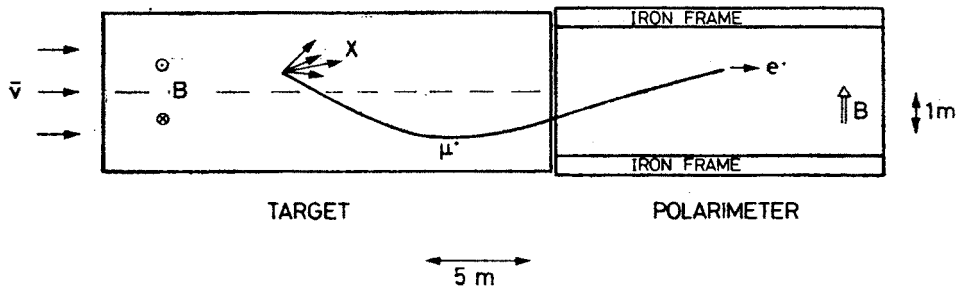


Fig. 1. Layout of the experiment to measure the polarization of muons produced in $\bar{\nu}_\mu N \rightarrow \mu^+ X$ (CDHS-CHARM experiment)

focuses the μ^+ towards the polarimeter. Approximately 5% of the muons stop inside the polarimeter and decay by $\mu^+ \rightarrow e^+ \bar{\nu}_\mu \nu_e$. The V-A structure of this decay process provides a relation between the muon spin direction and the e^+ emission angle. High-energy e^+ are emitted preferentially in the direction of the muon spin. This results in a forward-backward asymmetry, as shown in Fig. 2.

The iron frame around the polarimeter is magnetized in such a way as to produce, inside the polarimeter volume, a uniform magnetic field (58 G) transverse to the polarimeter axis. This field causes the muon spin to precess in a plane perpendicular to the marble

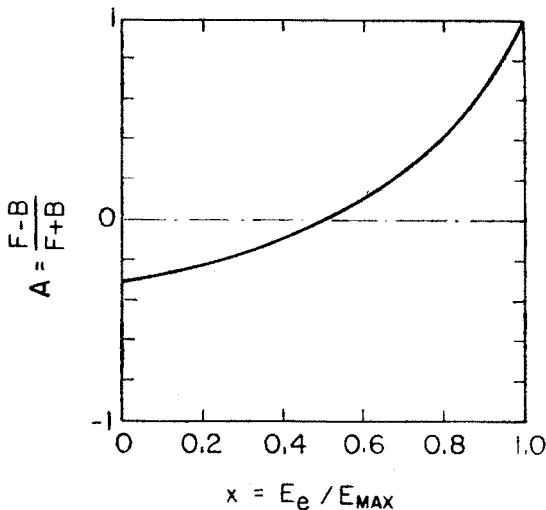


Fig. 2. Angular asymmetry $(F-B)/(F+B)$, of positron emission in muon decay as a function of fractional positron energy $x = E_e/E_{\max}$

plates. The positron yield detected in the forward or backward scintillator planes relative to the stopping position of the muon (Fig. 3) is thus periodically modulated:

$$N_{B,F}(t) = N_0 e^{-t/\tau} [1 \pm R_0 \cos(\omega t + \phi)],$$

which results in an oscillation pattern

$$R(t) = \frac{N_B(t) - N_F(t)}{N_B(t) + N_F(t)} = R_0 \cos(\omega t + \phi).$$

The phase ϕ describes the sign of the polarization ($\phi = 0$ for negative polarization, $\phi = -\pi$ for positive polarization), and the amplitude R_0 is proportional to the magnitude of the polarization ($R_0 = \alpha P$, α = polarimeter analysis power).

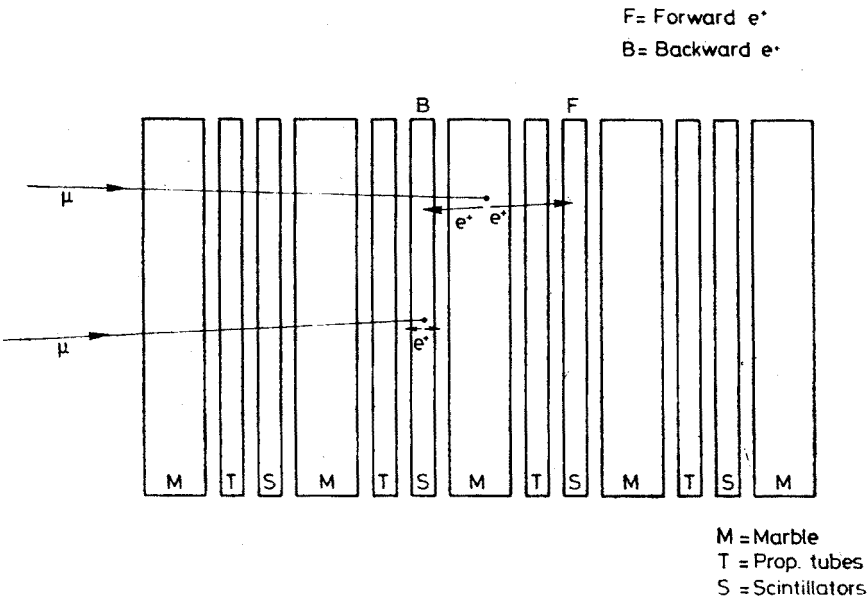


Fig. 3. Schematic view of the polarimeter structure with examples of μ^+ stopping and decaying in marble and in scintillator (CHARM apparatus)

TABLE II

Average values of some kinematical quantities characterizing the events used for the polarization analysis

$\langle p_\mu \rangle$	$= 16.1 \pm 0.4 \text{ GeV}/c$
$\langle E_\nu \rangle$	$= 26.5 \pm 0.9 \text{ GeV}$
$\langle E_x \rangle$	$= 10.2 \pm 0.8 \text{ GeV}$
$\langle x \rangle$	$= 0.19 \pm 0.01$
$\langle y \rangle$	$= 0.34 \pm 0.01$
$\langle Q^2 \rangle$	$= 3.2 \pm 0.3 (\text{GeV}/c)^2$

Data have been analysed corresponding to 20% of the full data sample and result in 13,000 stopping muons and 3400 accepted decay positrons. The average values of some kinematical quantities characterizing these events are listed in Table II. The resulting oscillation pattern $R(t)$ is shown in Fig. 4. Owing to the fact that muons stop also in the scintillators (in this case the positron is always assigned to the backward direction), the oscillation is not centred around $R = 0$.

The fit to the oscillation pattern $R(t)$ results in $R_0 = 0.14 \pm 0.2$ and $\phi = -3.1 \pm 0.2$. This phase value shows that the helicity is positive. To determine the absolute value of the

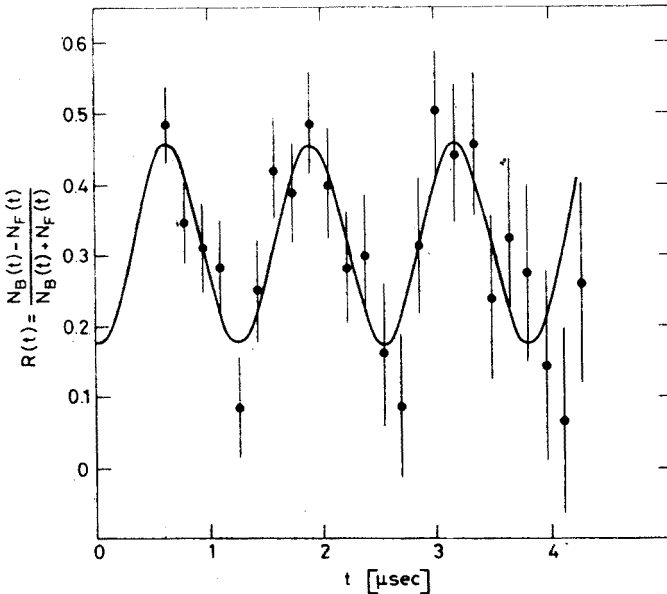


Fig. 4. Observed time dependence of relative backward-forward positron asymmetry. The sinusoidal function is the best fit to the experimental points (CDHS-CHARM data)

polarization P it is necessary to know the polarimeter analysis power α . This was determined by simulating, in a Monte Carlo calculation, the muon decay with the geometry of the polarimeter structure, taking into account the acceptance cut in the e^+ energy spectrum due to the finite marble thickness. The calculation gives the polarization as $P = +(1.09 \pm 0.22)$. This result confirms the V, A nature of the leptonic charged current at high momentum.

3. Neutral current experiments

The neutral current interactions are represented by the triangle shown in Fig. 5. The interactions are then given by all possible current \times current products, including the product of a current with itself.

The self-product of the neutrino current describes neutrino-neutrino scattering, which will hardly ever be seen. Weak neutral quark-quark scattering adds to small admix-

tures of opposite parity in nuclear states which give rise to observable parity-violating effects. The situation in the self-coupling of charged leptons, since the advent of e^+e^- colliding-beam machines such as PETRA and PEP, has progressed rapidly. The weak scattering processes such as $e^+e^- \rightarrow e^+e^-$, $\mu^+\mu^-$, and $\tau^+\tau^-$ are becoming observable. The very first results on this type of process have recently been published. Their significance

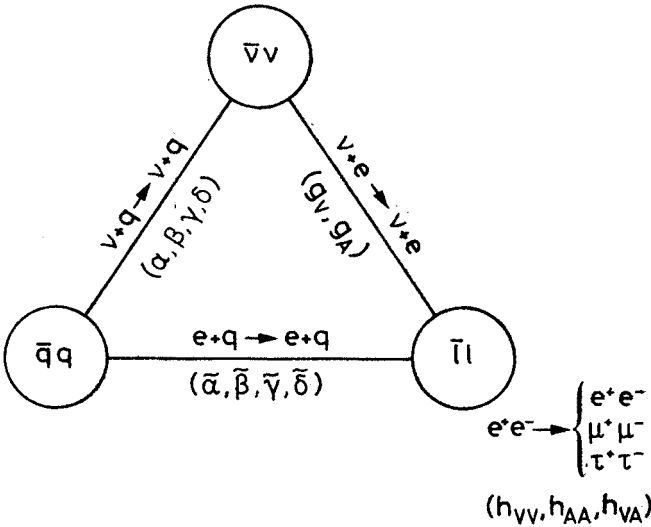


Fig. 5. Schematic representation of neutral current interactions

is as yet marginal, but the exploration of neutral currents with e^+e^- colliding beams will be of ever increasing importance in the years to come.

All existing experimental information on the structure of weak neutral currents stems from processes where the currents from two different sectors are employed: the most precise data have been obtained in neutrino-quark scattering and in electron-quark scattering. The cleanest process is neutrino-electron scattering, because no uncertainty about hadronic structure is involved. Unfortunately, the precision obtained so far is low, compared to that of neutrino quark or charged lepton-quark diffusion.

The ratio R_{ff} of the cross-section of the reaction $e^+e^- \rightarrow f\bar{f}$ to the point-like QED cross-section $\sigma_p = 4\pi\alpha^2/3s$, is given by (Ellis and Gaillard 1976)

$$R_{ff} = Q_f^2 - 8sgQ_f g_V g_{Vf} \frac{1}{(s/M_Z^2 - 1) + \Gamma_Z^2/(s - M_Z^2)} + 16s^2 g^2 (g_V^2 + g_A^2) (g_{Vf}^2 + g_{Af}^2) \frac{1}{(s/M_Z^2 - 1)^2 + \Gamma_Z^2/M_Z^2},$$

where Q_f is the charge, and g_{Vf} and g_{Af} are the vector and axial-vector coupling constants of the final-state fermion f . The constant g is defined by

$$g = \frac{G}{8\sqrt{2}\pi\alpha} = 4.47 \times 10^{-5} \text{ GeV}^{-2}.$$

At energies far below the resonance ($s \ll M_Z^2$), the deviation from the QED point-like cross-section is in good approximation given by the interference term only, and thus proportional to $g_V g_{V_f}$. Thus, for example, in the process $e^+e^- \rightarrow \mu^+\mu^-$, one measures essentially the square of the vector coupling constant. In the context of the standard model, one will interpret the absence of a deviation from the QED prediction as $g_V^2 \cong 0$, or equivalently $\sin^2 \theta_w \cong 0.25$, which makes the vector coupling constant vanish.

A second measurable quantity is the forward-backward asymmetry of the process $e^+e^- \rightarrow f\bar{f}$. The asymmetry A is defined as

$$A = \frac{F - B}{F + B},$$

where F and B denote the differential cross-section of the $\mu^-(\tau^-)$, integrated over the forward and backward hemispheres with respect to the incident e^- . The asymmetry is given by

$$A_{ff} = \frac{6\chi(-Q_f g_A g_{A_f} + 8\chi g_V g_{V_f} g_A g_{A_f})}{Q_f^2 - 8Q_f \chi g_V g_{V_f} + 16\chi^2 (g_V^2 + g_A^2) (g_{V_f}^2 + g_{A_f}^2)},$$

with

$$\chi = g s \frac{M_Z^2}{s - M_Z^2}.$$

The decay width Γ_Z , being small as compared to M_Z , has been set to zero. Again, at energies far below the resonance, the asymmetry is in good approximation given by

$$A_{ff} \cong -6\chi Q_f g_A g_{A_f}.$$

For the process $e^+e^- \rightarrow \mu^+\mu^-$, for example, the asymmetry is proportional to the square of the axial-vector coupling constant:

$$A_{\mu\mu} \cong 6\chi g_A^2.$$

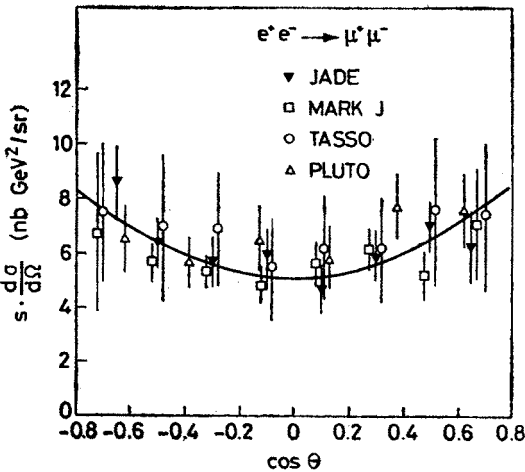


Fig. 6. The differential cross-section $d\sigma/d\cos\theta$ of the process $e^+e^- \rightarrow \mu^+\mu^-$. The full line shows the pure QED prediction

This yields an asymmetry of -9.6% at $\sqrt{s} = 35\text{ GeV}$, with $g_A^2 = 0.25$. This is within reach of the experiments, while the expected change in $R_{\mu\mu}$ is only 7×10^{-4} , unobservable at present energies.

The differential cross-section of the process $e^+e^- \rightarrow \mu^+\mu^-$ as a function of $\cos \theta$ (θ being the angle between the outgoing μ^- and the incident e^-) obtained by the various PETRA

TABLE III
Summary of forward-backward asymmetry measurements

	JADE	MARK J	PLUTO	TASSO
$A_{\mu\mu}$ meas.	-5 ± 6	-1 ± 6	7 ± 10	7 ± 7
$A_{\mu\mu}$ theor.	-6.6	-7.7	-5.8	-6.6
$\langle A_{\mu\mu} \rangle$ meas.	-2.8 ± 3.4			
$\langle A_{\mu\mu} \rangle$ theor.	-6.7			
$A_{\tau\tau}$ meas.		-6 ± 12		0 ± 11
$A_{\tau\tau}$ theor.		-7.0		-7.5
$\langle A_{\tau\tau} \rangle$ meas.	-3 ± 8			
$\langle A_{\tau\tau} \rangle$ theor.	-7.2			

groups (Wiik 1980, Böhm 1981) is shown in figure 6. The data are consistent with a $(1 + \cos^2\theta)$ distribution as expected from QED. No significant forward-backward asymmetry is observed, which allows upper limits to be placed on g_A^2 or, more precisely, on $g_A^e g_A^\mu$. The 95% upper confidence limit is $|g_A| < 0.56$ for the worst case $M_Z = \infty$.

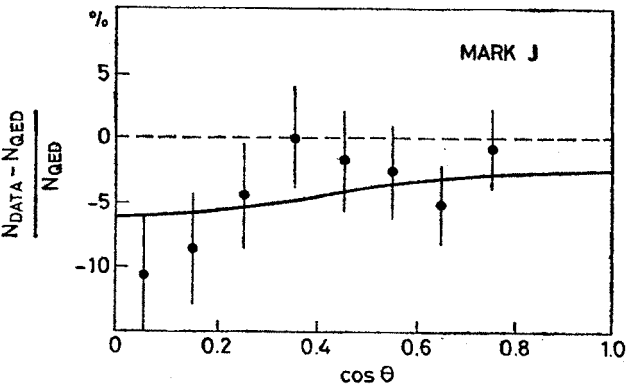


Fig. 7. The deviation from the QED prediction for the differential cross-section $d\sigma/d\cos \theta$ of the process $e^+e^- \rightarrow \mu^+\mu^-$. The full line represents the best fit to the standard electroweak model ($g_V^2 = -0.05, g_A^2 = 0.21$)

Similar results have been obtained from the process $e^+e^- \rightarrow \tau^+\tau^-$. The results of the asymmetry measurements are listed in Table III.

The relative deviation of the Bhabha cross-section due to weak effects is plotted in figure 7 as a function of the scattering angle (MARK J data, Barber et al. 1981). Although the data are consistent with the QED prediction, the best fit favours the presence of a weak effect consistent with the standard model ($g_V^2 = -0.05$, $g_A^2 = 0.21$). Similar analyses have

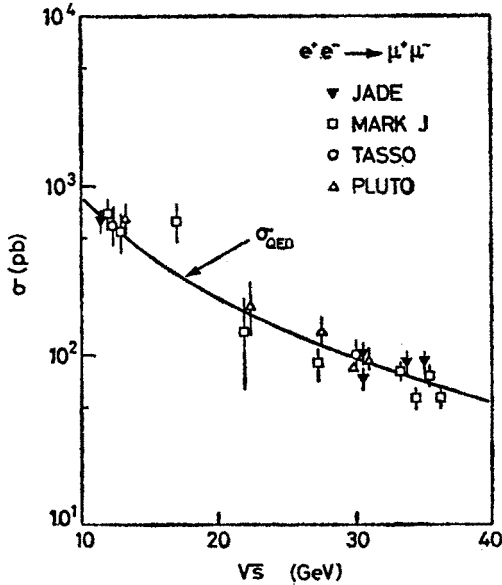


Fig. 8. Cross-section for $e^+e^- \rightarrow \mu^+\mu^-$ as a function of \sqrt{s} (GeV). The full line shows the pure QED prediction

been carried out by the CELLO, JADE, PLUTO and TASSO Collaborations (Böhm 1981, Bartel et al., 1981, Berger et al., 1981).

The cross-section for $e^+e^- \rightarrow \mu^+\mu^-$ from various PETRA groups is shown in figure 8 as a function of \sqrt{s} . The observed cross-section is consistent with the QED point-like cross-section and is also in line with the expectation from the standard model which predicts an unobservably small deviation from QED. The measurement shows, according to formula of R_{ff} , that there is no unexpectedly large vector coupling constant involved.

The constraints on g_V^2 and g_A^2 from e^+e^- experiments can be combined with the information obtained from νe scattering experiments. The allowed region from MARK J data (Barber et al., 1981) is shown in figure 9. The e^+e^- experiments favour clearly the solution with axial-vector dominance, which coincides with the prediction of the standard model.

Using the standard model the data $e^+e^- \rightarrow e^+e^-$, $e^+e^- \rightarrow \mu^+\mu^-$, and $e^+e^- \rightarrow \tau^+\tau^-$ can be used to extract values of $\sin^2 \theta_W$. The resulting values for $\sin^2 \theta_W$ are listed in Table IV, together with the type of experimental data which have been used.

While there is no doubt that the present results from e^+e^- interactions cannot yet compete with the precision achieved in neutrino-quark scattering experiments, the e^+e^- results are obtained at substantially larger values of Q^2 ($\sim 1000 \text{ GeV}^2$), and involve all

known charged leptons. The fact that the data constrain the vector coupling constant to a value close to zero is a non-trivial result.

Recently, the analysis of R has been extended by the JADE (Bartel et al., 1981) and the MARK J (Barber et al., 1981) Collaborations to $R(e^+e^- \rightarrow q\bar{q} \rightarrow \text{hadrons})$. The under-

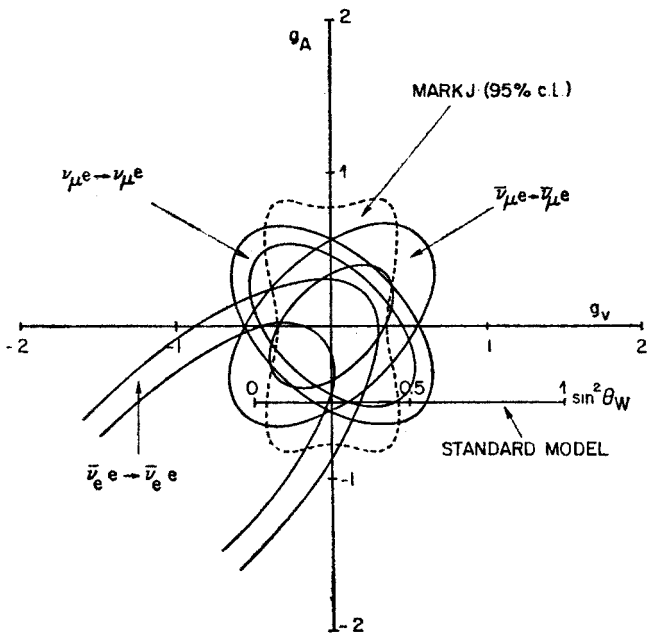


Fig. 9. Allowed domains for g_V and g_A as determined from neutrino-electron scattering, and from $e^+e^- \rightarrow l^+l^-$ ($l = e, \mu, \tau$)

lying assumption is that five quark flavours (u, d, c, s, b) describe correctly the data in the energy range $12 < \sqrt{s} < 36.7 \text{ GeV}$, and resonant effects are absent. It has been argued that this constitutes a test of the standard model in a new domain of large Q^2 and in processes which involve the production of quarks of all three generations.

TABLE IV

Summary of determinations of $\sin^2 \theta_W$ from purely leptonic reactions at PETRA

	$\text{Sin}^2 \theta_W$	Source of information
CELLO	0.25 ± 0.15^a	R_{ee}
JADE	0.25 ± 0.15	$R_{ee}, R_{\mu\mu}, A_{\mu\mu}$
MARK J	0.24 ± 0.12	$R_{ee}, R_{\mu\mu}, R_{\tau\tau}, A_{\mu\mu}$
PLUTO	0.22 ± 0.22	$R_{ee}, R_{\mu\mu}, R_{\tau\tau}, A_{\mu\mu}$
TASSO	0.24 ± 0.11^a	$R_{ee}, A_{\mu\mu}$

^a Preliminary.

Of course, it would be of great interest to study the weak coupling constants of all known quark flavours and to compare them with the predictions of the standard model. In practice, this cannot be done at present energies. One is forced to assume that all quarks have the couplings as predicted by the standard model, and the only free parameter is then $\sin^2 \theta_w$. The dependence of $R(e^+e^- \rightarrow q\bar{q})$ on $\sin^2 \theta_w$ is shown in figure 10, and it

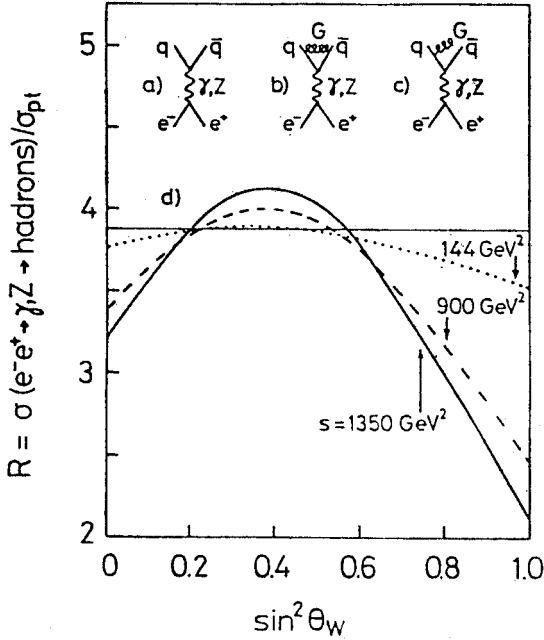


Fig. 10. The variation of the ratio of the total cross-section $\sigma(e^+e^- \rightarrow q\bar{q})$ to the point-like QED cross-section, as a function of $\sin^2 \theta_w$. The horizontal line at $R = 3.87$ corresponds to single γ exchange only (Bartel et al., 1981)

can be seen that, in the context of the standard model, a negative result of the search for weak effects in $R(e^+e^- \rightarrow q\bar{q})$ — as is the case — constrains $\sin^2 \theta_w$ to values around 0.23. The JADE result for $\sin^2 \theta_w$ is 0.22 ± 0.08 , and the MARK J result is $\sin^2 \theta_w = 0.27^{+0.34}_{-0.08}$. The main message of the experiment is, however, that at large Q^2 apparently none of the quarks has an unexpectedly large coupling strength.

4. Neutrino scattering on isoscalar nuclei

Inclusive neutral-current reactions on (nearly) isoscalar targets allow the most precise measurement of neutral-current couplings. The measured quantities are the ratios of the inclusive neutral- to charged-current cross-sections R_ν and $R_{\bar{\nu}}$, and the y distribution ($y = E_{\text{had}}/E_\nu$). The latter gives, when interpreted in the framework of the quark-parton model, information on the Lorentz structure of hadronic neutral currents.

The theoretical analysis of the measured quantities assumes in first approximation that the neutrino scatters off free quarks. It has been shown in high-precision experiments

from the analysis of charged-current events that the quark-parton model is indeed a very good approximation for the internal structure of the nucleon. Today's precision is such that all relevant deviations from the simple quark-parton model, like scaling violation of the structure functions and the amount of the non-strange and strange sea as a function of Q^2 , are reasonably well known (uncertainties from this sector are comparable or small compared to experimental errors of neutral-current studies).

Since almost all precision in the determination of neutral-current parameters comes from neutrino scattering on isoscalar nuclei, it seems appropriate to recall here the results of a recent fit to all available data on neutral-current phenomena, performed by Kim et al. (1980). Their aim was to determine as fully as possible the structure of the hadronic and leptonic neutral current without recourse to the standard electroweak model, to search for the effects of small deviations from the standard model, and finally to determine in the context of the standard model the value of $\sin^2 \theta_w$ as accurately as possible.

The first aim is accomplished by fitting a number of phenomenological coupling constants, assuming only vector and axial-vector covariants for the Lorentz structure of the neutral current, and isovector and isoscalar pieces only for the isospin components of the neutral hadronic current. It turns out that all resulting coupling constants are consistent with the values predicted by the standard model. For details, we refer to the report of Kim et al. (1980).

Next, Kim et al. tried a fit of a generalized $SU(2) \times U(1)$ model, where the third component of the weak isospin of the right-handed fermions is kept as a free parameter. The results of this fit are:

$$\begin{aligned} \text{Fit 1: } \varrho &= 1.018 \pm 0.045, & I_{3R}^u &= -0.010 \pm 0.040, \\ \sin^2 \theta_w &= 0.249 \pm 0.031, & I_{3R}^d &= -0.101 \pm 0.058, \\ & & I_{3R}^e &= 0.039 \pm 0.047. \end{aligned}$$

A deviation of $\varrho = M_W^2/(M_Z^2 \cos^2 \theta_w)$ from unity would indicate a more complicated Higgs structure than just a doublet of scalar particles. Apparently, there is no need for more than the minimal structure. The third components of the weak isospin of the u_R and d_R quarks, and the e_R electron, are consistent with zero, indicating that the assignment of right-handed fermions as singlets under weak isospin is correct. The next fit is therefore done setting $I_{3R}^u = I_{3R}^d = I_{3R}^e$ to zero.

$$\begin{aligned} \text{Fit 2: } \varrho &= 1.002 \pm 0.015, \\ \sin^2 \theta_w &= 0.234 \pm 0.013. \end{aligned}$$

We notice that ϱ remains consistent with one, with very good accuracy. This is in line with the standard model which predicts $\varrho = 1$ of the first order. Therefore, a third fit is performed assuming the strict validity of the standard model, with only $\sin^2 \theta_w$ as a free pa

$$\text{Fit 3: } \sin^2 \theta_w = 0.233 \pm 0.009 \ (\pm 0.005).$$

The error given in brackets reflects an estimate of theoretical uncertainties in the extraction of $\sin^2 \theta_w$ out of experimental data.

Undoubtedly, the agreement of all recent experimental data constitutes a triumph for the standard model. However, looking in a little bit more detail at the global fit to the existing data, three caveats may be appropriate:

(i) In the theoretical analysis, as well as in all experimental analyses, weak and electromagnetic corrections have ignored throughout.

(ii) The fit to all available experiments to get the best value of $\sin^2 \theta_W$ can be criticized because the quoted experimental errors are usually not Gaussian, making a χ^2 minimization doubtful.

(iii) The errors quoted by Kim et al. (1980) are apparently correlated errors and not uncorrelated errors which are normally quoted as results of multiparameter fits. This is shown in figure 11, which gives the correlation ellipse for the fit of ρ and $\sin^2 \theta_W$ (Fit 2). The correlation ellipse is taken from a similar fit performed by Roos and collaborators

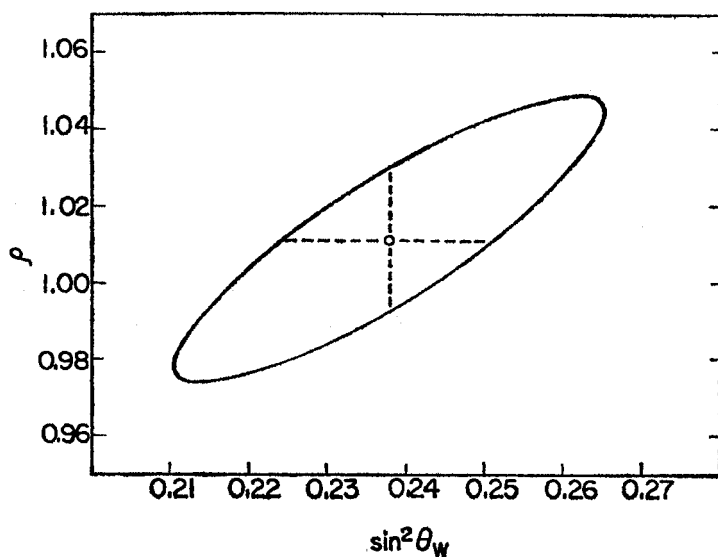


Fig. 11. Correlation ellipse in two parameter fit of ρ and $\sin^2 \theta_W$

(1981). The immediate result of the quotation of correlated errors is that the probability of the correct solution lying within the quoted errors is significantly less than 68%. Recent results on neutral current from a single experiment (CHARM) avoid the problem of combined experimental data from various and give

$$R_\nu = 0.320 \pm 0.009 (\pm 0.003 \text{ syst.}),$$

$$R_{\bar{\nu}} = 0.377 \pm 0.020 (\pm 0.003 \text{ syst.}),$$

with a hadron energy cut-off of only 2 GeV. Using the same QCD model calculation as Kim et al., a value of

$$\sin^2 \theta_W = 0.220 \pm 0.014$$

is deduced (the error does not cover theoretical uncertainties of the model calculation). The new results are in good agreement with previous measurements (see figure 12).

The experiments on neutrino-quark interactions have achieved a high degree of experimental accuracy and the determination of the fundamental quantity $\sin^2 \theta_w$ is close, in these experiments, to the uncertainty due to the theoretical corrections in computing the hadronic final states. The purely leptonic experiments and the Z_0 mass can improve the determination of the second coupling constant of the gauge theory of the weak interaction $SU(2)_L \times U(1)$.

In the preparation of these lectures I have extensively used two beautiful reviews of weak interactions: one by J. Meyer (CERN EP Internal Report 80-09, 9 December 1980),

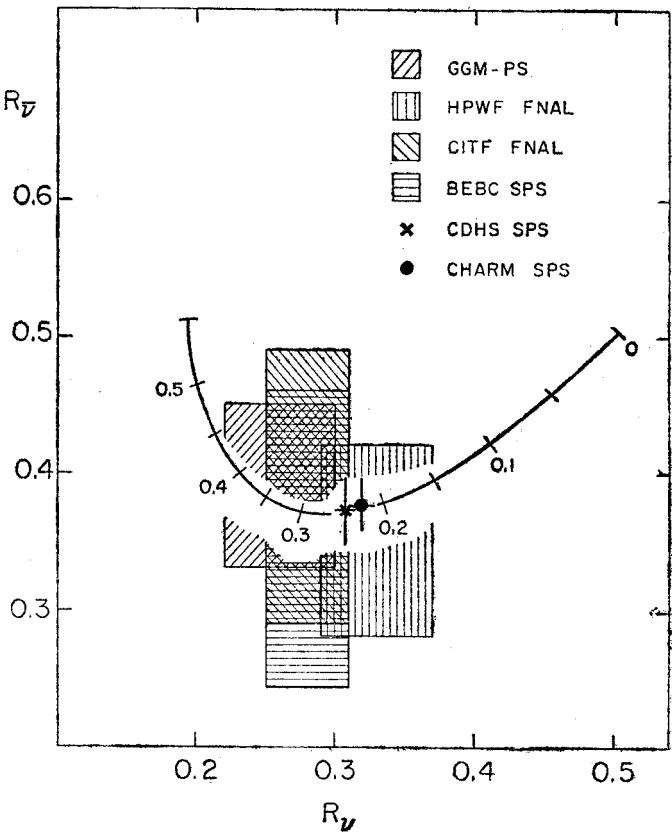


Fig. 12. Comparison of the results of various experiments on R_ν and $R_{\bar{\nu}}$ with the standard model and the other by F. Dydak (Invited talk given at the Royal Society Discussion Meeting on Gauge theories of the fundamental interactions, London, 29-30 April 1981). I recommend that students should read these reviews in order to gain a more complete view of the experimental situation in the field of weak interactions.